

General Disclaimer

One or more of the Following Statements may affect this Document

- This document has been reproduced from the best copy furnished by the organizational source. It is being released in the interest of making available as much information as possible.
- This document may contain data, which exceeds the sheet parameters. It was furnished in this condition by the organizational source and is the best copy available.
- This document may contain tone-on-tone or color graphs, charts and/or pictures, which have been reproduced in black and white.
- This document is paginated as submitted by the original source.
- Portions of this document are not fully legible due to the historical nature of some of the material. However, it is the best reproduction available from the original submission.

NASA Technical Memorandum 86913

(NASA-TM-86913) ON LOCA: TOTAL STRAIN
REDISTRIBUTION USING A SIMPLIFIED CYCLIC
INELASTIC ANALYSIS BASED ON AN ELASTIC
SOLUTION (NASA) 16 p HC A02/MF A01 CSCL 20K

N85-21690

G3/39 14611
Unclas

On Local Total Strain Redistribution Using a Simplified Cyclic Inelastic Analysis Based on an Elastic Solution

Shoi Y. Hwang
*South Carolina State College
Orangeburg, South Carolina*

and

Albert Kaufman
*Lewis Research Center
Cleveland, Ohio*

Prepared for the
Twenty-first Joint Propulsion Conference
cosponsored by the AIAA, SAE and ASME
Monterey, California, July 9-11, 1985

NASA



ON LOCAL TOTAL STRAIN REDISTRIBUTION USING A SIMPLIFIED CYCLIC INELASTIC ANALYSIS

BASED ON AN ELASTIC SOLUTION*

Shoi Y. Hwang
South Carolina State College
Orangeburg, South Carolina

and

Albert Kaufman
National Aeronautics and Space Administration
Lewis Research Center
Cleveland, Ohio 44135

Abstract

Strain redistribution corrections were developed for a simplified inelastic analysis procedure to economically calculate material cyclic response at the critical location of a structure for life prediction purposes. The method was based on the assumption that the plastic region in the structure is local and the total strain history required for input can be defined from elastic finite-element analyses. Cyclic stress-strain behavior was represented by a bilinear kinematic hardening model. The simplified procedure has been found to predict stress-strain response with reasonable accuracy for thermally cycled problems but needs improvement for mechanically load-cycled problems.

This study derived and incorporated Neuber-type corrections in the simplified procedure to account for local total strain redistribution under cyclic mechanical loading. The corrected simplified method was exercised on a mechanically load-cycled benchmark notched plate problem. Excellent agreement was found between the predicted material response and nonlinear finite-element solutions for the problem. The simplified analysis computer program used 0.3 percent of the CPU time required for a nonlinear finite-element analysis.

Introduction

Nonlinear, finite-element computer codes are generally too costly to use as a design tool for hot section components of aircraft gas turbine engines. Computing costs are further increased by the presence of high thermal gradients and geometrical irregularities, such as cooling holes. Most hot section components are of such geometrical complexity as to necessitate three-dimensional analyses, frequently with substructuring. Three-dimensional, nonlinear finite-element analyses are prohibitively time consuming and expensive to conduct in the early design stages for combustor and turbine structures. To improve the durability of these components, it is necessary to develop simpler and more economical methods for representing the structural response of materials under cyclic loading.

*Similar material will be presented in Local Strain Redistribution Corrections for a Simplified Inelastic Analysis Procedure Based on an Elastic Finite - Analysis by Albert Kaufman and Shoi Y. Hwang (NASA TP-2421).

A program has been underway at NASA Lewis to develop a simplified procedure¹⁻³ for performing nonlinear structural analysis using only an elastic finite element solution or strain gage data as input. Development of the simplified method was based on the assumption that the inelastic regions in the structure are constrained by the surrounding elastic material. This implies that the total strain history can be defined by an elastic analysis. Initial development of the method did not account for any strain redistribution. A computer program (ANSYMP) was created to predict the stress-strain history at the critical fatigue location of a thermomechanically cycled structure from elastic input data. Appropriate material stress-strain and creep properties and plasticity hardening models were incorporated into the program. Effective stresses and equivalent plastic strains are approximated by an iterative and incremental solution procedure. Creep effects can be obtained on the basis of stress relaxation at constant strain, cumulative creep at constant stress or a combination of stress relaxation and creep accumulation.

The simplified procedure has been found to predict critical location stress-strain response with reasonable accuracy relative to nonlinear finite-element analyses for thermally cycled problems.⁴ However, the limitation of no strain redistribution is most likely to be violated in the case of mechanically loaded structures, especially in the vicinity of stress concentrations. Nonlinear finite-element analyses of notched plate specimens subjected to cyclic mechanical loading have shown that the total strain range at the critical location can be significantly larger than would be predicted from elastic solutions.

This study derived and incorporated corrections in the simplified procedure to account for local total strain redistribution and residual stresses due to mechanical load cycling. These corrections would remove some of the limitations and extend the applicability of the procedure. The corrections were based on the Neuber rule⁵ relating the theoretical stress concentration factor to the actual stress and strain concentration factors.

Two variations of a benchmark notched plate problem⁶ were analytically examined to verify the accuracy of the improved simplified method. Verification was made through comparison with three-dimensional nonlinear, finite-element analyses. Cyclic stress-strain and creep properties for Inconel 718 alloy, a kinematic hardening model and

the von Mises yield criterion were used for the benchmark notch specimen problems. Elastic and elastic-plastic finite element analyses were performed using the MARC nonlinear finite-element computer code.⁷ The elastic solutions for the critical locations were used as input data for the simplified analysis computer code. Verification of the improved simplified procedure was made on the basis of how well it was able to duplicate the stress-strain hysteresis loops from MARC elastic-plastic analyses of the benchmark notch problem.

Nomenclature

e	nominal total strain at net section
E	modulus of elasticity
E_e	modified modulus of elasticity
E_p	work hardening slope (Fig. 1)
$K_{\epsilon n}$	temperature-dependent constants in cyclic stress-strain equation
K_t	theoretical elastic stress or strain concentration factor
K_{ϵ}	actual strain concentration factor
K_{σ}	actual stress concentration factor
S	effective nominal elastic stress at nth increment
S^*	effective local elastic stress (real or imaginary)
S_m^*	maximum effective local elastic stress
ϵ	equivalent total strain, unmodified
ϵ^*	equivalent total strain, modified
ϵ_e	uncorrected equivalent elastic strain
ϵ_p	equivalent plastic strain
ϵ_p^i	maximum equivalent plastic strain in cycle (Fig. 1)
ϵ_R	equivalent local residual strain
σ	effective stress (loading), unmodified
σ^i	maximum effective stress in cycle (Fig. 1)
σ_2	effective stress (unloading), unmodified
σ^*	effective stress (loading), modified
σ_2^*	effective stress (unloading), modified
σ_m	maximum effective stress, unmodified
σ_m^*	maximum effective stress, modified
σ_R	local residual stress
σ_{yi}	initial yield stress in loading part of cycle

σ_{yi}	initial yield stress in unloading part of cycle
μ	Poisson's coefficient

Analytical Procedure

Improvements were made to a simplified inelastic procedure for calculating the stress-strain history at the critical fatigue location of a structure subjected to cyclic thermomechanical loading. The basic assumption in the initial development of the procedure was that the inelastic region is local and constrained from redistribution by the surrounding elastic material. It follows from this assumption that the total strain history at the critical location can be defined by an elastic solution. Justification for the assumption of elastic constraint of local inelasticity can be found in finite element analyses of thermally cycled structures,⁸⁻¹¹ such as combustor liners, aircooled turbine blades, and wedge fatigue specimens which have shown that the total strain ranges from elastic and nonlinear solutions are in close agreement. However, this assumption is invalid for structures subjected mainly to mechanical load cycling, as was shown¹ for the benchmark notch problem.

In this study, a strain redistribution factor (SRF) was derived to account for local total strain redistribution under applied cyclic loads. This correction also accounted for residual strains induced by plastic yielding. The strain redistribution factor is applied to the ideal local total strain obtained from the elastic solution. These corrections were incorporated in a version of the ANSYMP program using a kinematic hardening model to characterize the yield surface under cycling. A representation of a cyclic stress-strain curve by a bilinear kinematic hardening model is illustrated in Fig. 1. The loci of the tips of the cyclic curves is described by the relation

$$\sigma = K(\epsilon_p)^n \quad (1)$$

The work hardening slope, E_p , for the kinematic hardening model was determined from energy considerations to give the same strain energy, as indicated by the enclosed area in Fig. 1, as the actual stress-strain curve. This work hardening slope will be defined by

$$E_p = \left(\frac{\sigma^i}{\epsilon_p^i} \right) \left(\frac{2n}{1+n} \right) \quad (2)$$

The von Mises criterion was used, thereby converting the total strain from a uniaxial stress-strain curve into a modified equivalent total strain.¹² This modified elastic part of the equivalent total strain corresponds to the measured elastic strain multiplied by $2(1+\mu)/3$. This relationship must be taken into account in a multi-axial stress-strain field when applying results from elastic finite-element analyses. As a result, all stresses and strains from the elastic solution are expressed in terms of von Mises effective stress and modified equivalent total strain; these values are assigned signs based on the dominant

principal stress and strain directions. For computational convenience, the factor $2(1 + \nu)/3$ was included in the elastic modulus and the modified elastic modulus will be designated by E_e where $E_e = 3/(2(1 + \nu))E$.

The elastic input data are subdivided into a sufficient number of increments to define the stress-strain cycle. Dwell times are specified for increments which require creep analysis. The increments are analyzed sequentially to obtain the cumulative plastic and creep strains and to track the yield surface. An iterative process is used to calculate the yield stresses for increments undergoing plastic straining. First, an estimated plastic strain is assumed for calculating an initial yield stress from the stress-strain properties and the simulated hardening model. Second, a new plastic strain is calculated as the difference between the total strain and the elastic and creep strain components. The yield stress is then recalculated using the new plastic strain. This iterative process is repeated until the new and previous plastic strains agree within a tolerance of 1 percent.

Neuber's rule for approximating local stresses and strains in the plastic region was used as the basis for the development of the strain redistribution corrections. With minor modifications, this rule provides acceptable predictions of local stresses and strains in the loading part of a stable cycle and less accurate predictions in the unloading part of the cycle. The relative failure of Neuber's rule for the unloading part of the cycle has been mainly due to neglect of the local residual stresses. Regardless of the part of the cycle being studied, an adjustment must be made to the stresses to account for the work hardening slope of the cyclic stress-plastic strain curve.

The strain redistribution analysis for the stable cycle is divided into three stages; elastic-plastic loading, elastic unloading and plastic unloading. Figure 2 is presented to further define the symbols used in the governing equations for each of these stages.

Elastic-Plastic Loading

Neuber's rule specifies a relationship between the theoretical stress concentration factor, K_t , and the actual stress concentration factor, K_σ , and the actual strain concentration factor, K_ϵ , of the form

$$K_t^2 = K_\sigma K_\epsilon \quad (3)$$

Substituting local and net section stresses and strains into Eq. (3) gives

$$K_t^2 = \left(\frac{\sigma}{S}\right)\left(\frac{\epsilon}{e}\right) \quad (4)$$

where K_t also equals S^*/S or $\sigma = S^2/(\epsilon E_e)$.

The cyclic stress-strain relation is assumed to take the form

$$\sigma = E_e \epsilon \quad \text{when} \quad \epsilon \leq \sigma_{yi}/E_e \quad (5)$$

or

$$\sigma = \left(1 - \frac{E_p}{E_e}\right) \sigma_{yi} + E_p \epsilon \quad \text{when} \quad \epsilon \geq \frac{\sigma_{yi}}{E_e} \quad (6)$$

Combining Eqs. (4) to (6) gives the local strain as

$$\epsilon = \frac{(-B + \sqrt{B^2 + C})}{A} \quad (7)$$

where

$$A = 2E_p$$

$$B = \left(1 - \frac{E_p}{E_e}\right) \sigma_{yi}$$

$$C = 4 \left(\frac{E_p}{E_e}\right) S^{*2}$$

The local stresses and strains calculated by using the work hardening slope in Eqs. (6) and (7) have to be modified to account for the elastic strain change between σ and σ_{yi} . The modified local stress, σ^* , corresponding to the local strain, ϵ^* , can be expressed as

$$\sigma^* = \left(\frac{E_p}{E_e}\right) \sigma_{yi} + \left(1 - \frac{E_p}{E_e}\right) \sigma \quad (8)$$

and the modified local strain, ϵ^* , as

$$\epsilon^* = \epsilon - \frac{(\sigma - \sigma^*)}{E_e} \quad (9)$$

The plastic strain, ϵ_p at the stress level σ^* is

$$\epsilon_p = \epsilon^* - \frac{\sigma^*}{E_e} \quad (10)$$

To relate the ideal local inelastic strain to the local total strain, a strain redistribution factor (SRF) is introduced. The SRF at the nth increment on the stress-strain curve can be written as

$$(\text{SRF})_n = \epsilon_n^* - \frac{S_n^*}{E_e} \quad (11)$$

To improve the accuracy of the predicted local stress-strain history, a strain redistribution factor, SRF, was generated for each increment during the loading part of the cycle. This SRF represents the cumulative total strain correction up to the nth point on the stress-strain curve. Therefore, the total strain at that increment is the uncorrected elastic strain, ϵ_e , for that increment plus the sum of all the incremental SRFs up to that increment.

$$\epsilon_n^* = \epsilon_{en} + \sum_{i=1}^n [(\text{SRF})_i - (\text{SRF})_{i-1}] \quad (12)$$

Equation (12) is another way of expressing ϵ^* given in Eq. (9).

Elastic Unloading

The local stress at the nth increment in the elastic unloading part of the cycle (Fig. 2) is simply

$$\sigma_n = \sigma_m^* - (S_m^* - S_n^*) \quad (13)$$

and the corresponding local total strain is

$$\epsilon_n = \epsilon_m^* - \frac{S_m^* - S_n^*}{E_e} \quad (14)$$

or expressed in a form similar to Eq. (12)

$$\epsilon_n = \epsilon_{en} + \sum_{i=1}^n [(SRF)_i - (SRF)_{i-1}] \quad (15)$$

For an isothermal problem where an incremental approach is not required, Eq. (15) can be simplified to $\epsilon_n = \epsilon_{en} + (SRF)_m$.

Inelastic Unloading

Upon complete removal of the applied load, residual stresses remain across the net section. Denoting the local residual stress as σ_R , then

$$\sigma_R = \sigma_m^* - S_m^* \quad (16)$$

and the complimentary local residual strain, ϵ_R , is

$$\epsilon_R = \frac{\sigma_R}{E_e} \quad (17)$$

Again the cyclic stress strain relation in the plastic region is assumed to take a linear form

$$\sigma = \left(1 - \frac{E_p}{E_e}\right) \sigma'_{yi} + E_p \epsilon \quad (18)$$

As a kinematic hardening model is used in the analysis, the new initial yield stress is given by

$$\sigma'_{yi} = \sigma_m^* - 2\sigma_{yi} \quad (19)$$

Considering the zero stress and plastic strain at σ_m^* the new origin, as shown in Fig. 2, the local stress and total strain can be expressed as

$$\sigma = K_\sigma S + \sigma_R \quad (20)$$

and

$$\epsilon = K_\epsilon e + \epsilon_R \quad (21)$$

Combining Eqs. (3), (18), (20), and (21) leads to the solution for

$$\epsilon = \frac{[-A - \sqrt{A^2 + B}]}{(2E_p)} \quad (22)$$

where
$$A = \left(1 - \frac{E_p}{E_e}\right) \sigma'_{yi} - E_p \epsilon_R - \sigma_R$$

$$B = 4E_p \left[\left(1 - \frac{E_p}{E_e}\right) \sigma'_{yi} \epsilon_R + \frac{S_m^{*2}}{E_e} - \sigma_R \epsilon_R \right]$$

The actual local stresses and strains are obtained by a series of iterations between the modified and unmodified values. Two iterations, as shown below, have been found sufficient to give an acceptably convergent solution. Iterations do not appear to be necessary for the loading part of the cycle. The modified local stress, σ_2^* , corresponding to ϵ^* is expressed as

$$\sigma_2^* = \left(\frac{E_p}{E_e}\right) \sigma'_{yi} + \left(1 - \frac{E_p}{E_e}\right) \sigma_2 \quad (23)$$

where σ_2 is obtained from the following steps

$$\sigma = \left(1 - \frac{E_p}{E_e}\right) \sigma'_{yi} + E_p \epsilon \quad (24)$$

$$\sigma^* = \left(\frac{E_p}{E_e}\right) \sigma'_{yi} + \left(1 - \frac{E_p}{E_e}\right) \sigma \quad (25)$$

$$\epsilon_1 = \epsilon - \frac{(\sigma - \sigma^*)}{E_p} \quad (26)$$

$$\sigma_1 = \left(1 - \frac{E_p}{E_e}\right) \sigma'_{yi} + E_p \epsilon_1 \quad (27)$$

$$\sigma_1^* = \left(\frac{E_p}{E_e}\right) \sigma'_{yi} + \left(1 - \frac{E_p}{E_e}\right) \sigma_1 \quad (28)$$

$$\epsilon_2 = \epsilon - \frac{(\sigma_1 - \sigma_1^*)}{E_p} \quad (29)$$

$$\sigma_2 = \left(1 - \frac{E_p}{E_e}\right) \sigma'_{yi} + E_p \epsilon_2 \quad (30)$$

and the modified local total strain, ϵ^* , as

$$\epsilon^* = \epsilon - \frac{\sigma - \sigma_2}{E_p} - \frac{\sigma_2 - \sigma_2^*}{E_e} + \epsilon_p \quad (31)$$

The plastic strain, ϵ_p , at the stress level

σ_2^* is

$$\epsilon_p = \frac{\epsilon^* - \sigma_2^*}{E_e} \quad (32)$$

The strain redistribution factor at the nth increment on the stress-strain curve is

$$(SRF)_n = \epsilon_n - \frac{\sigma_n - \sigma_{n2}}{E_p} - \frac{\sigma_{n2} - \sigma_{n2}^*}{E_e} - \frac{S_n^* + \sigma_R}{E_e} \quad (33)$$

or, in terms of the uncorrected elastic strain, the total strain at the nth increment can be written as

$$\epsilon_n^* = \epsilon_{en} + (SRF)_m - \sum_{i=1}^n [(SRF)_i - (SRF)_{i-1}] \quad (34)$$

$$\text{where} \quad (\text{SRF})_m = \epsilon_m - \frac{S_m^*}{E_e} - \frac{\sigma_m - \sigma_m^*}{E_e}$$

Equation (34) is simply another form of expressing ϵ^* previously given in Eq. (31).

Another version of the ANSYMP computer program was created to implement the improved simplified analytical procedure. The program consists of the main executive routine, ANSYMP, and four subroutines, ELAS, YIELD, CREEP, and SHIFT. The incremental elastic data and temperatures are read into subroutine ELAS. Material stress-strain properties as a function of temperature and a simulated hardening model are incorporated in subroutine YIELD and the creep characteristics are incorporated in subroutine CREEP. Subroutine SHIFT is required to update the temperature effects on the yield stress shift. SHIFT also serves the function of deciding the future direction of the yield surface under nonisothermal conditions by determining the relation of future to past thermal loading.

The calculational scheme initially follows the effective stress-equivalent strain input data from subroutine ELAS until the occurrence of initial yielding. The stress-strain solution then proceeds along the yield surface as determined from the stress-strain properties in subroutine YIELD. At each increment during yielding the stress shift (difference between new yield stress and stress predicted from elastic analysis) from the original input data is calculated. Elastic load reversal is signaled when the input stress is less than the yield stress from the previous increment. During elastic unloading, the stresses are translated from the original elastic analysis solution by the amount of the calculated stress shift. Reverse yielding occurs when the stress reaches the reverse yield surface as determined from the hardening model incorporated in subroutine YIELD. Again, the solution follows the yield surface until another load reversal is indicated when the stress based on the shifted elastic solution is less than the yield stress. The elastic response during load reversal is obtained by translating the original elastic solution according to the new stress shift calculated during reversed yielding. The stress-strain response for subsequent cycles is computed by repeating this procedure of identifying load reversals, tracking reverse yield surfaces and translating the original elastic solution during elastic loading and unloading. Creep computations are performed for increments involving dwell times using the creep equation and strain hardening rule incorporated in subroutine CREEP. Depending on the nature of the problem, the creep effects are determined on the basis of one of the three options provided in the subroutine.

The code will automatically avoid the Neuber-type strain redistribution corrections for thermal loading problems where there are no applied mechanical loads. Without applied loads, the Neuber method would be inapplicable since Eq. (4) would have zero net stresses and strains in the denominator. Provision is also made for the user to circumvent the corrections for other situations where they should not be taken into account. These situations include locally strain controlled problems and, as will be shown, problems where the total strain input is based on strain measurements rather than elastic finite-element analyses.

Since the stable cyclic stress-strain curve is a function of the plastic strain range, it is necessary to iterate between the maximum plastic strain used to specify the stress-strain curve and the analytical solution. In both the MARC code and the original ANSYMP code, this required rerunning the problem until the assumed and calculated plastic strains were in reasonable agreement. In the improved version of the ANSYMP program, the iteration was automated so that the analysis was repeated using the previously calculated maximum plastic strain to define the stress-strain curve. This iterative process is continued until the specified and calculated maximum plastic strains agree within 10 percent, usually within three iterations.

The computer program was verified by conducting simplified analyses for the benchmark notch problem and comparing the results to those from MARC nonlinear analyses. The geometry of the benchmark notch specimen is illustrated in Fig. 3. This specimen was tested under isothermal conditions as part of a program to provide controlled strain data for constitutive model verification.⁶ A MARC analysis of this problem using kinematic hardening demonstrated excellent agreement with experimental data.⁴ Two variations of this problem were analyzed; one with the initial loading carried out to a plastic strain of 0.4 percent and the second with the specimen loaded to a maximum plastic strain of 0.6 percent with a small amount of strain ratcheting. A kinematic hardening model was used with cyclic stress-strain data for Inconel 718 alloy.⁶ Nonlinear and elastic MARC analyses of this problem were performed using approximately 600 triangular plane strain elements to model a quarter segment bounded by planes of symmetry as shown in Fig. 4. The MARC solutions shown for the benchmark notch specimen were computed at the closest Gaussian integration point to the root of the notch.

Discussion of Analytical Results

The results of the improved simplified inelastic analyses of the benchmark notch problems is discussed herein. Comparisons are made with MARC inelastic solutions. Stress-strain cycles used for comparison purposes are in terms of effective stresses and equivalent total strains using the von Mises yield criterion computed with signs based on the assigned signs in the original elastic solution. The entire discussion is based on the critical location at the notch root.

The benchmark notch test was conducted by mechanical load cycling at a constant temperature of 649 °C. A mechanically loaded structure, especially where the peak strain occurs at a stress raiser, is most likely to violate the basic assumption of the simplified approach that strain redistribution is prevented by containment of the local plastic region by the surrounding elastic material. It was shown¹ that the total strain range from the MARC elastic-plastic analysis was 20 percent greater than that obtained from the MARC elastic analysis. This foreshortening of the elastic strain range caused the simplified procedure to truncate the stress-strain hysteresis loop as shown in Fig. 5(a). When the input total strain history was based on optical strain measurements at the notch root, the agreement between the simplified and MARC elastic-plastic stress-strain hysteresis loops was good as demonstrated in Fig. 5(b). Both

the ANSYMP and MARC elastic-plastic analyses gave stable stress-strain hysteresis loops for the second cycle. It is to be noted that when the simplified analysis uses strain measurements rather than elastic finite-element solutions, strain redistribution corrections are unnecessary and should not be applied.

In Fig. 5(c) similar comparisons are shown using the simplified procedure corrected for strain redistribution on the loading part of the cycle and the MARC elastic solution as input. Neuber corrections for residual stresses and strain redistribution on the unloading part of the cycle were not implemented for this case. The truncation of the stress-strain hysteresis loop shown in Fig. 5(a) was eliminated and the ANSYMP solution showed good agreement with the MARC solution. This demonstrates the significant improvement in accuracy that can be attained by applying the Neuber correction in the plastic region, even without the residual stress correction during unloading.

When both the loading and unloading strain redistribution corrections were applied, the agreement between the predicted and MARC elastic-plastic results was even better, as shown in Fig. 5(d).

The original benchmark problem analyzed in Fig. 5, was a completely closed cycle and the maximum plastic strain was about 0.4 percent. To exercise the improved simplified procedure on an even more severe case, the mechanical loading was increased so that the plastic strain reached approximately 0.6 percent and strain ratchetting was induced. Again the agreement between the ANSYMP and MARC inelastic solutions was excellent, as shown in Fig. 6. It should be noted that the simplified procedure was able to capture the strain ratchetting on the second cycle.

The slight discrepancies between the the ANSYMP and MARC hysteresis loops in Figs. 5(d) and 6 were due primarily to the iteration process built into ANSYMP which resulted in the use of a cyclic stress-strain curve slightly different from that used in the MARC elastic-plastic analysis. The ANSYMP analyses of the benchmark notch problem used 0.3 percent of the central processor unit (CPU) time required by the MARC nonlinear analyses; this is without considering that the latter had to be run several times to obtain a cyclic stress-strain curve compatible with the calculated maximum plastic strain.

Summary of Results

An improved simplified analysis procedure was developed for calculating the stress-strain history at the critical location of a thermomechanically cycled structure. This improved procedure incorporated Neuber-type corrections to account for strain redistribution and residual stresses due to plastic strain reversals. Analytical predictions from the simplified procedure for benchmark notched plate problems were compared to nonlinear finite-element solutions. The following general conclusions were drawn from the evaluation of the method:

1. The predicted stress-strain response based on elastic finite-element solutions with the Neuber-type corrections showed excellent agreement with elastic-plastic finite-element solutions using the MARC program.

2. The predicted stress-strain response using only the corrections for plastic yielding on the loading part of the cycle showed good agreement with the MARC elastic-plastic solution. The corrections for the unloading part of the cycle were of secondary importance.

3. The strain redistribution corrections should not be applied when the input total strain history is based on local strain measurements rather than elastic finite-element analyses. It is also known from previous evaluations of the simplified procedure that these corrections should not be applied in thermal loading problems. For cases where a structure is subjected to a combination of thermal and mechanical loads, a method will have to be developed to partition the thermal and mechanical stresses so that the strain redistribution corrections are only applied to the mechanical stresses.

4. Stress-strain hysteresis loops were computed at the critical location on the structure using 0.3 percent of the CPU time required for elastic-plastic finite-element analyses.

References

1. Kaufman, A., "A Simplified Method for Nonlinear Structural Analysis," NASA TP-2208, 1983.
2. Kaufman, A., "Development of a Simplified Procedure for Cyclic Structural Analysis," NASA TP-2243, 1984.
3. Kaufman, A., "A Simplified Method for Elastic-Plastic-Creep Structural Analysis," NASA TM-84509, 1983.
4. Kaufman A., "Evaluation of Inelastic Constitutive Models for Nonlinear Structural Analysis," Nonlinear Constitutive Relations for High Temperature Applications, NASA CP-2271, 1983, pp. 89-106.
5. Neuber, H., "Theory of Stress Concentration for Shear-Strained Prismatical Bodies with Arbitrary Nonlinear Stress-Strain Law," Journal of Applied Mechanics, Vol. 28, No. 4, Dec. 1961, pp. 544-550.
6. Dumas, P.A., Sharpe, W.N., Ward, M., and Yau, J., "Benchmark Notch Test for Life Prediction," General Electric, Cincinnati, OH, R82AEBJ58, June 1982. (NASA CR-165571)
7. MARC General Purpose Finite Element Program, Vol. A: User Information Manual; Vol. B: MARC Element Library. MARC Analysis Research Corporation, Palo Alto, CA, 1980.
8. Moreno, V., "Combustor Liner Durability Analysis," General Electric, Cincinnati, OH, R81AEG372, Feb. 1982. (NASA CR-165250)
9. McKnight, R.L., Laflen J.H., and Spamer, G.T., "Turbine Blade Tip Durability Analysis," United Technologies Corp., East Hartford, CT, PWA-5684-19, Feb. 1981. (NASA CR-165268)
10. Kaufman A., and Hunt, L.E., "Elastic-Plastic Finite-Element Analyses of Thermally Cycled Double-Edge Wedge Specimens," NASA TP-1973, 1982.

11. Kaufman, A., and Gaugler, R.E., "Nonlinear, Three-Dimensional Finite-Element Analysis of Air-Cooled Gas Turbine Blades," NASA TP-1669, 1980.

12. Mendelson, A., Plasticity: Theory and Application, Macmillan, New York, 1968.

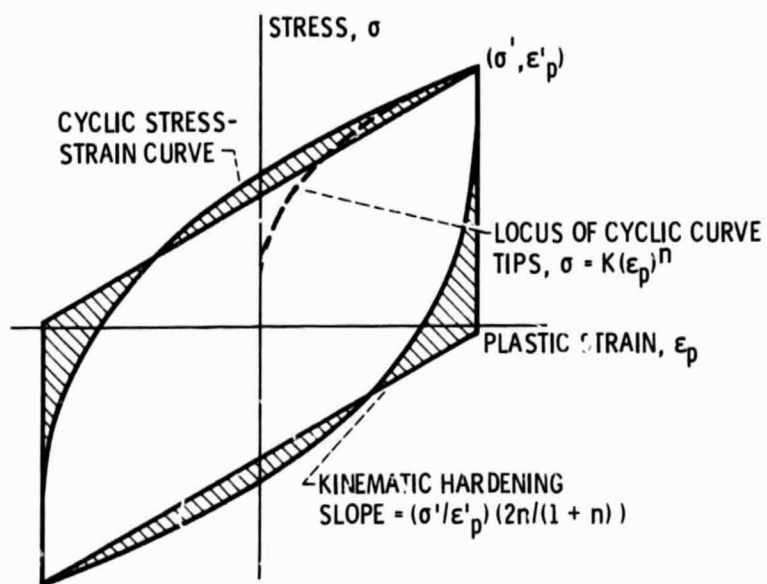
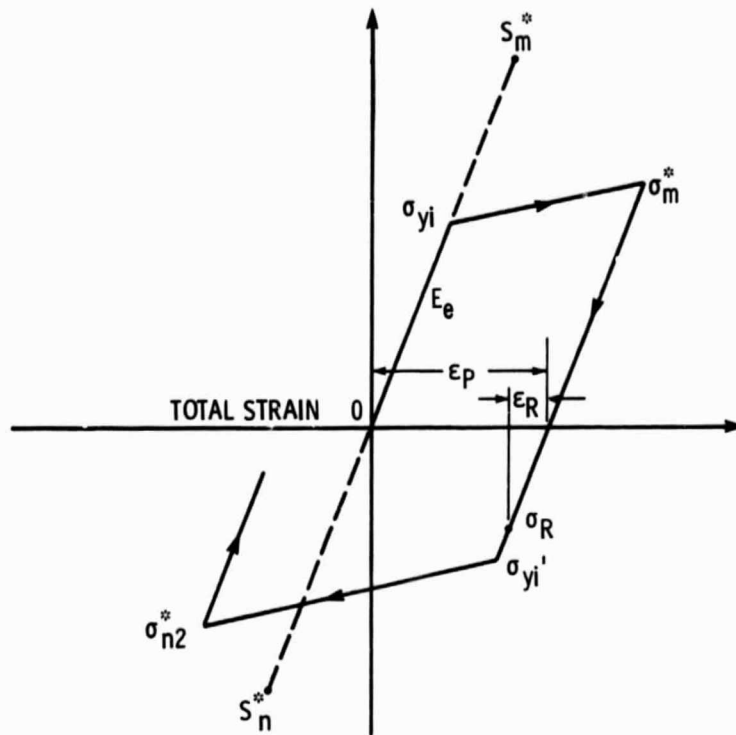
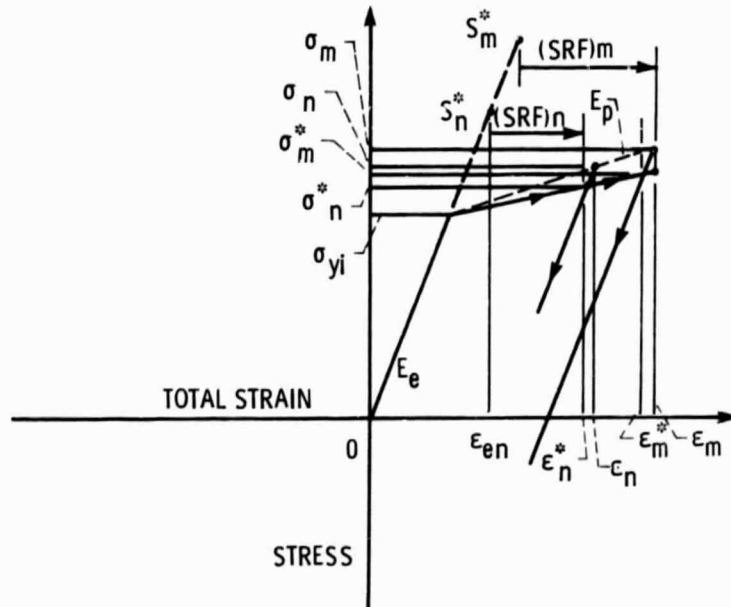


Figure 1. - Cyclic stress-strain representation.

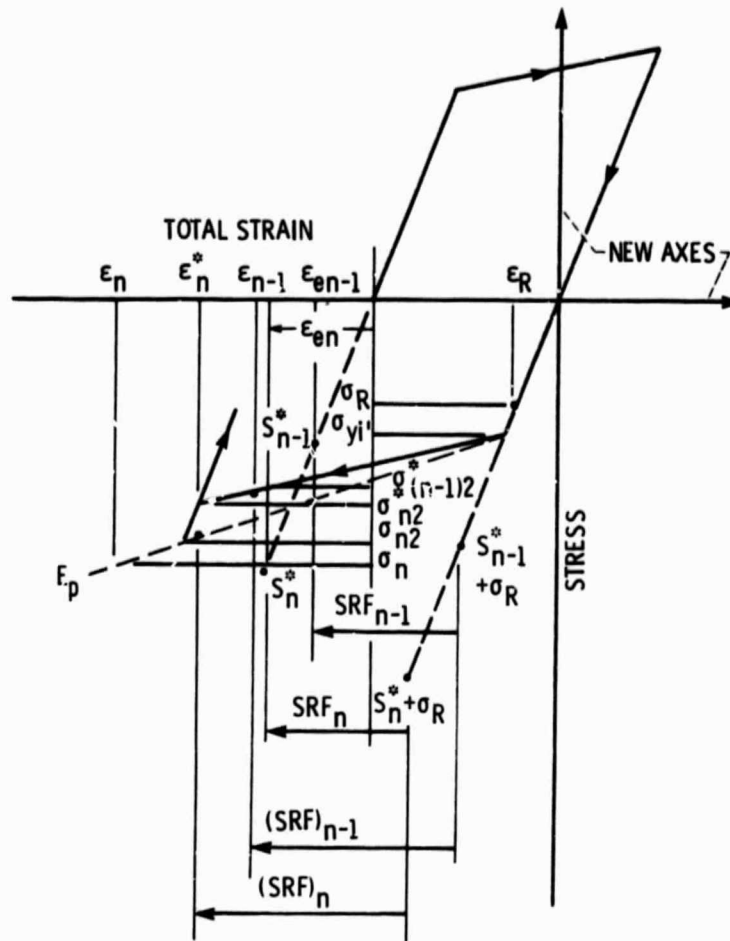


(a) Overall cyclic stress-strain response.



(b) Loading part of cycle.

Figure 2. - Description of symbols.



(c) Unloading part of cycle.

Figure 2. - Concluded.

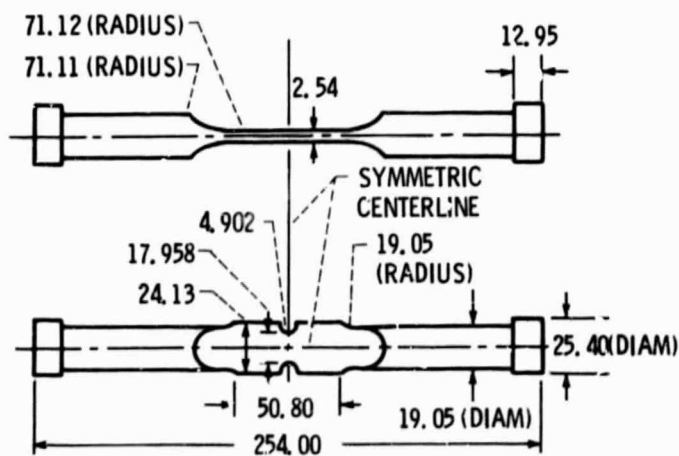


Figure 3. - Benchmark notch specimen ($\kappa_t = 1.9$). (All dimensions in mm.)

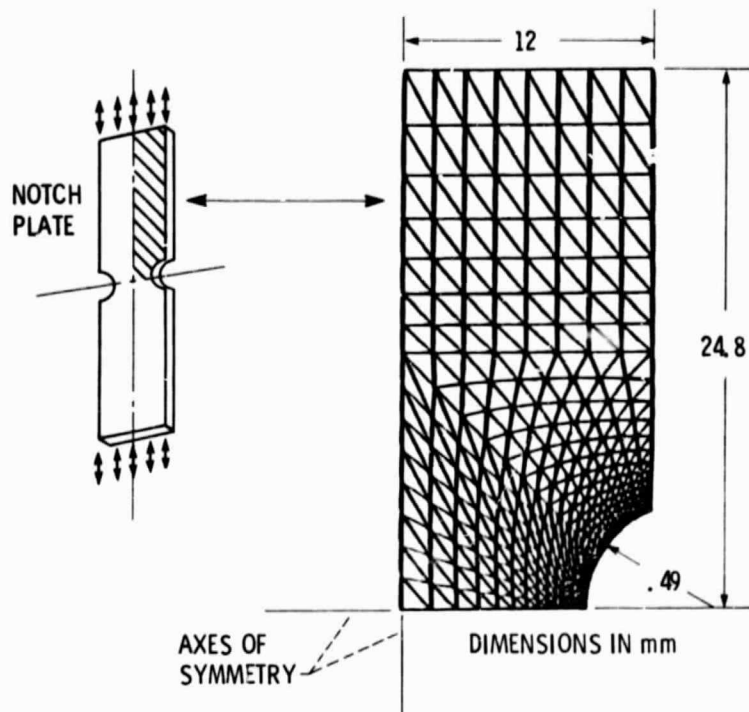


Figure 4. - Benchmark specimen finite-element model.

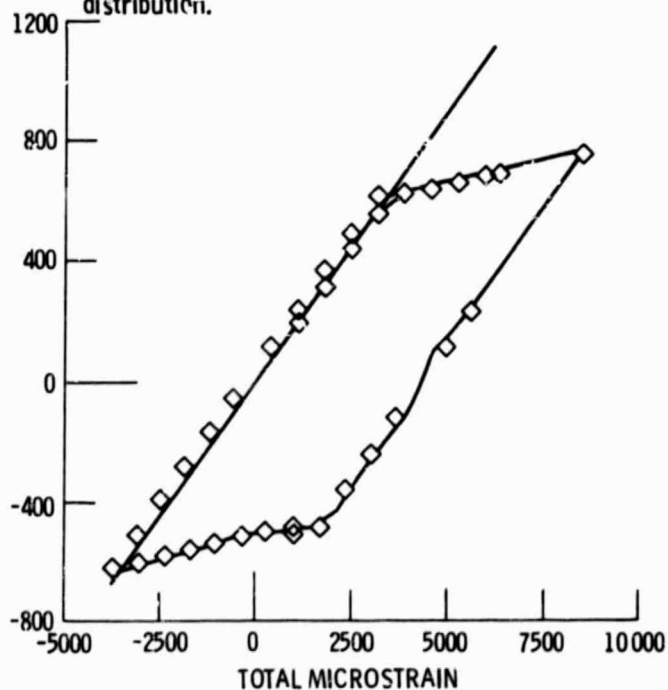
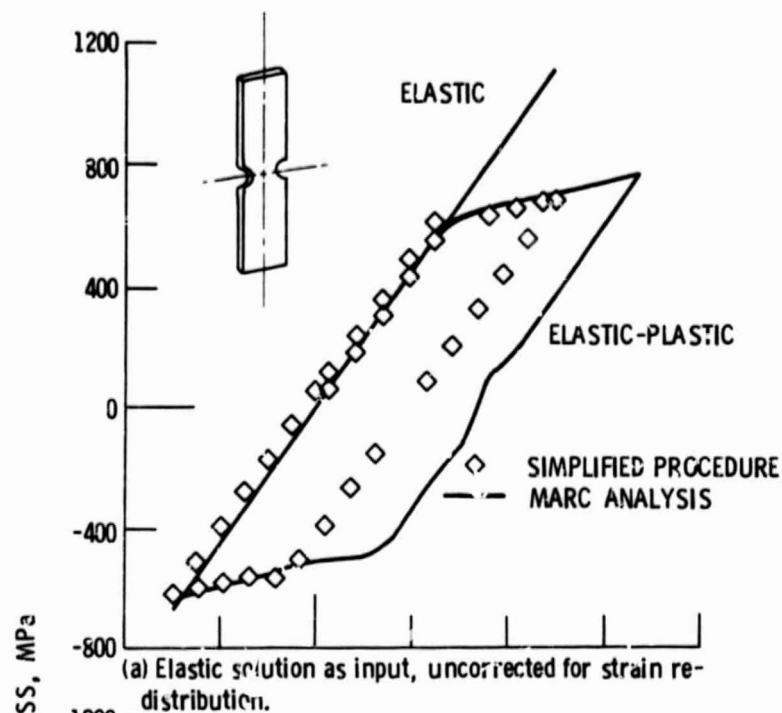
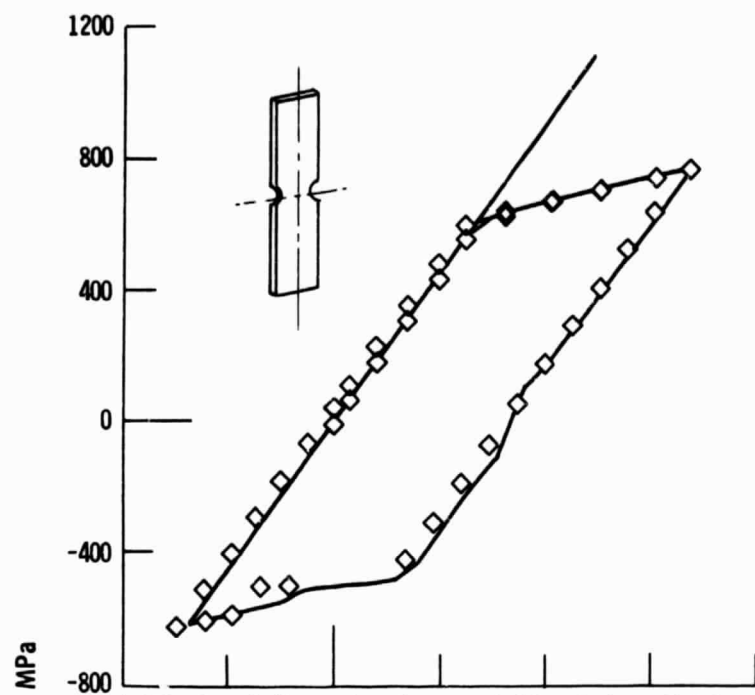
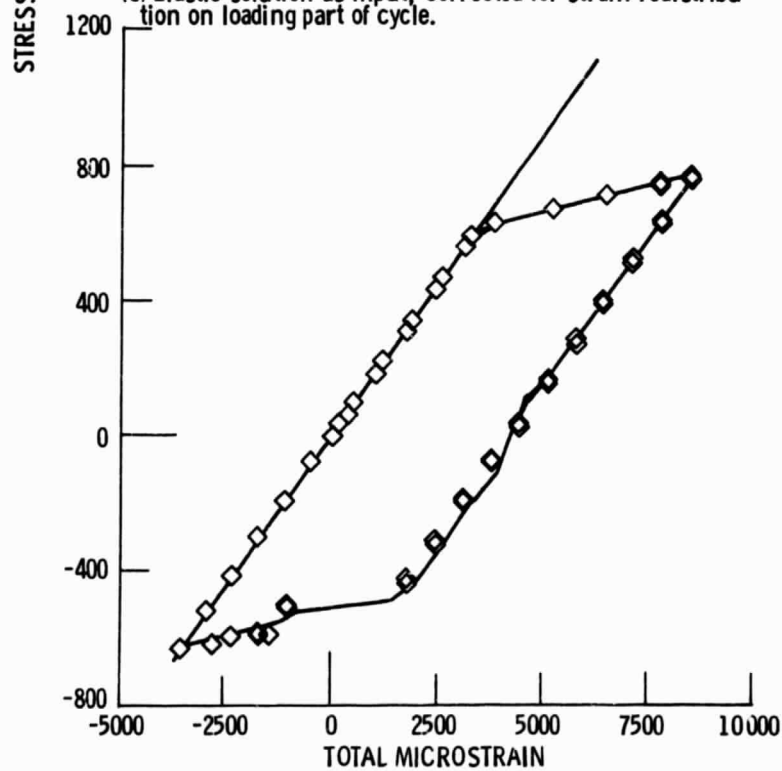


Figure 5. - Comparison of ANSYMP and MARC results for benchmark problem (0.4% maximum plastic strain).



(c) Elastic solution as input, corrected for strain redistribution on loading part of cycle.



(d) Elastic solution as input, corrected for strain redistribution on loading and unloading parts of cycle.

Figure 5. - Concluded.

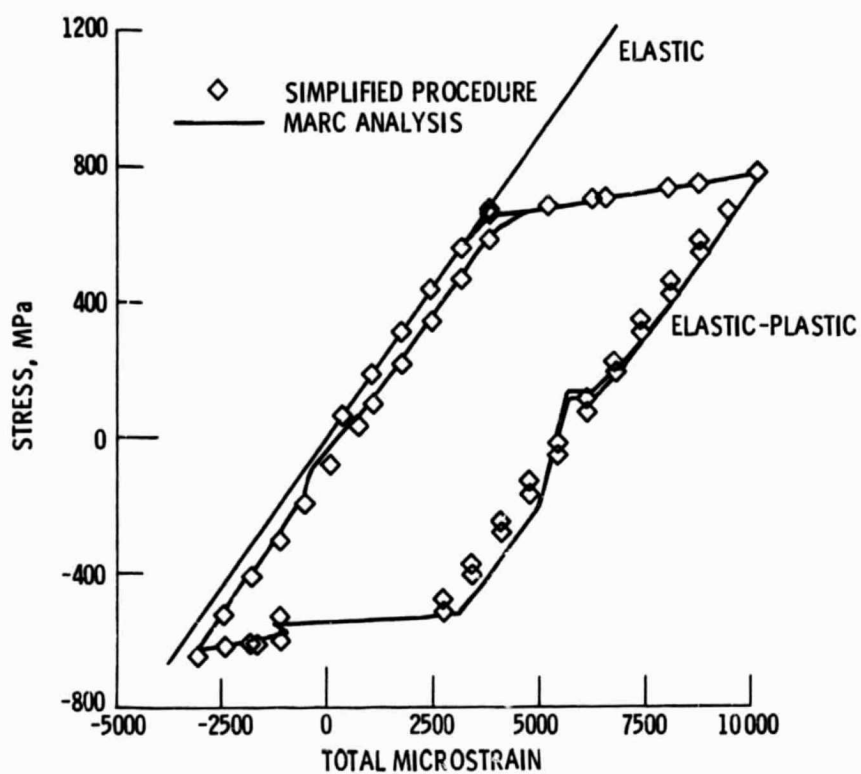


Figure 6. - Comparison of ANSYMP and MARC results for benchmark problem (0.6% maximum plastic strain).